Nuclear Medicine and Biology 61 (2018) 21–27

Contents lists available at ScienceDirect

Nuclear Medicine and Biology

journal homepage: www.elsevier.com/locate/nucmedbio

Imaging thrombosis with ^{99m}Tc-labeled RAM.1-antibody *in vivo*

Ali Ouadi [a,*], Virgile Bekaert [a], Nicolas Receveur [b,c,d], Lionel Thomas [a], François Lanza [b,c,d], Patrice Marchand [a], Christian Gachet [b,c,d], Pierre H. Mangin [b,c,d], David Brasse [a], Patrice Laquerriere [a]

[a] Université de Strasbourg, CNRS, IPHC UMR 7178, F-67000 Strasbourg, France
[b] UMR-S949, Inserm, Strasbourg, F-67065, France
[c] Etablissement Français du Sang-Alsace (EFS-Alsace), Strasbourg F-67065, France
[d] Université de Strasbourg, FMTS, Strasbourg, F-67065, France

ARTICLE INFO

Article history:
Received 7 September 2017
Received in revised form 1 February 2018
Accepted 13 March 2018
Available online xxxx

Keywords:
Antibodies
Thrombosis
Platelets
Single-photon emission computed tomography

ABSTRACT

Introduction: Platelets play a major role in thrombo-embolic diseases, notably by forming a thrombus that can ultimately occlude a vessel. This may provoke ischemic pathologies such as myocardial infarction, stroke or peripheral artery diseases, which represent the major causes of death worldwide. The aim of this study was to evaluate the specificity of radiolabeled Rat-Anti-Mouse antibody (RAM.1).

Methods: We describe a method to detect platelets by using a RAM.1 coupled with the chelating agent hydrazinonicotinic acid (HYNIC) conjugated to ^{99m}Tc, for Single Photon Emission Computed Tomography (SPECT). To induce platelet accumulation at a site of interest, we used a mouse model of $FeCl_3$ induced injury of the carotid artery. 90 min after *i.v.* injection of [^{99m}Tc][Tc(HYNIC)-RAM.1], biodistribution of the radiolabeled RAM.1 was assessed, SPECT imaging and histological analysis were performed on the mice that underwent $FeCl_3$-induced vessel damage.

Results: We demonstrated a quick and strong affinity of the radiolabeled RAM.1 for the platelet thrombus. Results clearly demonstrated the ability of this radioimmunoconjugate for detecting thrombi from 10 min post injection with an exceptional thrombi uptake. Using $FeCl_3$, the median ratio between the thrombus and the background was 12.4 (range 9.3–42.3) as compared to 1.0 (range: 0.86–2.7) $p < 0.05$ when using 0.9% NaCl.

Conclusion: Thanks to the high sensitivity of SPECT, we provided evidence that [^{99m}Tc][Tc(HYNIC)-RAM.1] represents a powerful tool to detect localized platelet thrombi which could potentially be used in humans. Because of the relative low cost and high sensitivity, these results encourage further study like the detection of non-induced thrombus and further developments toward clinical application. This is further supported by the fact that RAM.1 recognizes human platelets.

1. Introduction

Blood platelets are small anucleated cells that circulate freely in the bloodstream. They play a key role in hemostasis, which represents the physiological process leading to the arrest of bleeding. After a vessel wall injury, platelets adhere to the adhesive proteins exposed to the flowing blood, become activated and aggregate to form a plug that seals the breach [1]. The same responses can occur in a diseased artery presenting a stenosed atherosclerotic plaque. Erosion or rupture of such a plaque exposes thrombogenic materials leading to the recruitment of circulating platelets, which form a thrombus that can ultimately occlude the vessel. Such a phenomenon, called arterial thrombosis, results in life-threatening ischemic pathologies such as stroke and myocardial infarction which are leading causes of death worldwide [2]. Thrombosis is not exclusively an acute phenomenon but can occur repeatedly on a developing atherosclerotic plaque or in a vessel aneurysm, while being clinically silent [3]. Detection of such thrombotic events might be useful to clinicians to adapt therapeutic approaches preventing thrombo-embolic complications.

Because of the central role of platelets in thrombus formation, they represent a privileged target for thrombus imaging. Therefore, the detection of platelet accumulation is of major importance to detect thrombotic pathologies. Many strategies such as ultrasound, magnetic resonance imaging (MRI) or nuclear imaging techniques [4] were developed to image thrombus clinically and pre-clinically. McCarty and colleagues [5] proposed an indirect strategy based on ultrasound imaging allowing detection of activated Von Willebrand factor (VWF) following the injection of GPIb-coated microbubbles. Such an approach would not only detect VWF on activated platelets within thrombi, but also immobilized VWF on the vascular endothelium and therefore provide a non-invasive approach to image advanced prothrombotic and inflammatory phenotype in atherosclerotic disease. Several probes were

* Corresponding author at: Université de Strasbourg, IPHC, 23 rue du Loess, CNRS, UMR 7178, 67037 Strasbourg, France.
E-mail address: ali.ouadi@iphc.cnrs.fr (A. Ouadi).

https://doi.org/10.1016/j.nucmedbio.2018.03.003
0969-8051/

proposed to identify thrombi by targeting fibrin, activated platelets and factor XIII by molecular MRI [6–8]. One drawback of MRI is the low sensitivity of contrast agent detection compared to nuclear techniques. Indeed, nuclear imaging techniques such as positron emission tomography (PET) and single photon emission computed tomography (SPECT) provide excellent sensitivity allowing detection in the picomolar range. Recently the targeting of ^{99m}Tc radiolabeled fucoidan in rats allowing *in vivo* detection of P-selectin, such as an arterial thrombus has been evaluated [9]. Sequential whole-body acquisitions showed an early renal uptake of the tracer, followed by the bladder, with a high activity in urine, indicating a renal elimination of radiolabeled hydrophilic LMW fucoidan. Another study reported the use of an ^{111}In radiolabeled single-chain antibody targeting the LIBS epitope of activated integrin αIIbβ3, to selectively reveal platelet activation, and wall-adherent non-occlusive thrombosis in a mouse model [10]. Bitistatin, a single-chain disintegrin labeled with ^{123}I has also been used to locate thrombi and emboli by scintigraphic imaging [11]. Finally, monoclonal antibodies and small antibody fragments were radiolabeled and used for the sensitive detection of activated platelets and thrombosis [12]. In any cases, the ratio of radioactivity measured between the injury site containing the platelets and the surrounding tissue was modest. A ratio between 2 and 6 is not sufficient to clearly delineate a thrombosis.

In the present study, we proposed to use RAM.1, a rat monoclonal antibody reacting against mouse and human GPIbβ, a subunit of the GPIb-V-IX complex [13], and that was generated in our laboratory. This antibody was labeled with ^{99m}Tc to image thrombi *in vivo*. This complex is highly specific for platelets suggesting that such a strategy will detect non-moving platelets notably those present in a thrombus or in an aneurysm. RAM.1 is a particularly interesting antibody since it efficiently and specifically labels platelets as observed in immunofluorescence studies [1]. Moreover, it has already been used *in vivo*, in mice, and presented the potential to bind the human GPIb-V-IX complex [14].

We radiolabeled RAM.1 with ^{99m}Tc ($T_{1/2} = 6$ h) by conjugation with the chelating agent hydrazinonicotinic acid (HYNIC) to perform single photon emission SPECT imaging in mice. S-HYNIC, as developed by Abrams and coworkers [15], appears to be an ideal Bifunctional Chelating Agent (BCA) for ^{99m}Tc-labeling, due to its rapid and efficient labeling of antibodies. This approach consists of a conjugation step and a labeling step. In the conjugation step, S-HYNIC reacts with ε-amino groups of lysine residues in the antibody, resulting in a HYNIC-antibody conjugate. Conjugation of HYNIC to the antibody and optimal conditions (concentration of antibody, buffer solution and time) for radiolabeling the immuno-conjugate were determined, and the reactivity of the immunoconjugate to platelets was assessed by flow cytometry analysis. Formation of a platelet thrombus was achieved by using a well characterized $FeCl_3$-injury model of the mouse carotid artery [16]. Selective uptake of [^{99m}Tc][Tc(HYNIC)-RAM.1] in the thrombus of injured carotid artery was demonstrated by SPECT imaging.

2. Materials and methods

2.1. RAM.1 production and purification

P3.×63.Ag8.653 hybridoma cells expressing RAM.1 were generated as earlier described [13]. These cells were cultured in a RPMI 1640 medium containing 10% of FBS and 1% PSG. The supernatant of the culture was collected every 2–3 days and kept at 4 °C. Once a significant amount of supernatant was obtained, RAM.1 was purified by using a Prot G Hitrap column (GE Heathcare Lifescience, Pittsburgh, PA) as described earlier.

2.2. Conjugation of HYNIC to RAM.1

Two different buffer solutions were explored (1 M $NaHCO_3$ pH 8.2 and 0.1 M Borate buffer pH 8.5) to assess the effect of conjugation on labeling efficiency. Three different antibody concentrations were used (0.5 mg/mL, 8.7 mg/mL and 14 mg/mL). The reaction time was varied from 30 min to 120 min. Similar results were obtained when varying buffer solution and time reaction. The most important factor was the antibody concentration. At the lowest antibody concentration, virtually no HYNIC was conjugated to the antibody, and labeling efficiencies were therefore very low. More efficient conjugation and subsequent labeling was obtained at higher concentrations (8.7 mg/mL). Conjugation reaction failed when increasing antibody concentration (14 mg/mL). Optimum conjugation was obtained by incubating RAM.1 with S-HYNIC for 2 h in darkness using a 20:1 HYNIC/RAM.1 M ratio. These conjugation conditions (borate buffer, HYNIC/RAM.1 20:1, 2 h incubation time) were used for all further *in vitro* and *in vivo* experiments.

The monoclonal antibody RAM.1 was generated in our laboratory [13] and the rat IgG isotype control was obtained from Becton Dickinson (Le Pont de Claix, France). RAM.1 monoclonal antibodies were radiolabeled with ^{99m}Tc after bioconjugation with S-Hynic (succinimidylhydrazinonicotinamide, SynChem, Inc.). 320 μL of borate buffer (0.1 mol/L, pH 8.5) and 17 μL of a 1 mg/mL solution of S-Hynic in dimethylformamide (DMF) were added to a solution of RAM.1 (435 μg in 50 μL of phosphate buffer). Protected from light, the solution was stirred at room temperature for 2 h. A sodium citrate buffer solution (200 μL, 0.01 mol/L, pH 5.2) was added and the resulting solution was centrifuged at 13,000 RPM over 30,000 MW cutoff filtering devices (Amicon Ultra 0.5 mL centrifugal filters, Millipore).

The HYNIC conjugated RAM.1 antibodies were collected with 4 fold 75 μL of sodium citrate (0.01 mol/L, pH 5.2) and stored at 5 °C. An aliquot (20 μL) of this mother solution was used to determine the RAM.1 concentration (380 μg/mL) and to assess its affinity for platelets before radiolabeling.

2.3. Radiolabeling with ^{99m}Tc

6 μL of a freshly prepared hydrochloric (0.1 mol/L) solution of $SnCl_2$ (40 mg/mL) was added to 5 mL of an aqueous solution of tricine (36 mg/mL, Sigma-Aldrich Co, adjusted to pH 7.1 with NaOH 1 mol/L). 120 μL of this solution was transferred into a 2 mL eppendorf tube and 208 MBq (80 μL) of freshly eluted sodium pertechnetate ($Na^{99m}TcO_4$) was added. Technetium-99 m, as [$^{99m}TcO_4$]Na in physiological solution, was obtained from a ^{99}Mo/^{99m}Tc generator Elumatic® III (CisBio/IBA Molecular, France). The solution was allowed to react 10 min, before addition of 90 μL of the HYNIC conjugated RAM.1 solution (380 μg/mL) and 110 μL of NaCl (0.9%). After 15 min of reaction, the solution was diluted with 400 μL of NaCl (0.9%) and purified by centrifugation over 30,000 MW cutoff filters (Amicon Ultra 0.5 mL centrifugal filters pretreated with 40 μL of 0.9% NaCl) in order to remove the excess of free ^{99m}Tc-pertechnetate and uncoupled ^{99m}Tc-Tricine.

The radiolabeled antibody (77 MBq) solution was diluted in 300 μL of NaCl (0.9%). The resulting solution was used to prepare calibrated dose (10 MBq ± 1 in 100 μL of 0.9% sterile NaCl) for *in vivo* imaging.

The radiochemical purity was determined by thin-layer chromatography (Sigma-Aldrich, France) with 0.1 mol/L citrate buffer (pH 5.0) as the mobile phase phase for determination of the sum of $^{99m}TcO_4^-$ and the radiolabeled tricine (Rf = 1) and with ammonia:ethanol:water in a ratio of 1:2:5 for colloid determination. In the last phase, colloid remains at the origin, while the ^{99m}Tc-HYNIC–RAM.1 and possible impurities such as $^{99m}TcO_4^-$ or ^{99m}Tc-tricine moves to the top.

2.4. RAM.1 binding to platelets

To evaluate whether HYNIC-coupled RAM.1 is efficiently binding to platelets, washed human platelets prepared as previously described [17] were incubated with HYNIC-coupled RAM.1, with untreated RAM.1 (10 μg/mL) or with an IgG control antibody (10 μg/mL) for 10 min, before adding a FITC-conjugated goat-anti-rat antibody (1/100) for 10 min. Samples were finally diluted in 500 μL of the same buffer

and analyzed in a Gallios flow cytometer (Beckman Coulter, Eibelstadt, Germany). After decay of Tc-99 m, [^{99g}Tc]Tc-tricine-HYNIC-labeled RAM1 was also evaluated with the same manner to check the binding capability.

2.5. $FeCl_3$-injury thrombosis model

$FeCl_3$ induced thrombosis was performed as described earlier [16]. 8-week old mice were anesthetized with an intraperitoneal injection of ketamine (100 mg/kg) and xylazine (20 mg/kg). The common carotid arteries were exposed and vascular injury was induced by applying a Whatman filter paper saturated with 7% $FeCl_3$ in 0.9% NaCl (or 0.9% NaCl for control) to the left carotid artery for 2 min. Mice were assigned to either the RAM.1 or the control group. Experiments were done in blocks of 5 animals each. Mice in two groups had vascular injury and one group received saline as control.

2.6. RAM.1 affinity in vivo

The affinity of RAM.1 *in vivo* was evaluated by injection of 500 μg of rabbit IgG (non-specific antibody) right after the thrombus induction by $FeCl_3$ (ci below). 30 min later, 10 μg of RAM.1-488 nm were injected. The mice ($n = 5$) were perfused with 2.5% glutaraldehyde *via* cardiac puncture in the left ventricle using a 5-ml syringe with a 25-gauge needle. An incision in the right atrium allowed to remove blood, saline, and fixative. Vessel segments were dissected and were post-fixed in 4% paraformaldehyde overnight. The carotids were washed in phosphate-buffered saline, frozen in optimal cutting temperature embedding medium, and cross-sectioned.

2.7. Micro-SPECT/CT data acquisition and image processing

The imaging procedure was initiated immediately after induction of the thrombosis. 10 MBq of ^{99m}Tc-RAM.1 in sodium chloride (0.9%, 6 μg antibodies), pH ~7, were injected through the right jugular vein. Each dose was measured and recorded before and after injection to determine the exact injected dose. Micro-SPECT/CT acquisitions were performed using the multimodality imaging system developed in our institute [18,19]. Mice were placed supine on a bed and kept anesthetized using 1% isoflurane throughout the experiment. The bed was first moved in the micro-CT field of view (FOV). 360 X-ray projections were acquired over 360° at 40 kV and 75 μA with a total acquisition time of 42 s. The 256 × 512 × 720 (0.2 × 0.2 × 0.2 mm) micro-CT volume was reconstructed using Feldkamp algorithm implemented on GPU architecture. The mouse was then moved into the micro-SPECT FOV. Micro-SPECT images were acquired using the four-head gamma camera equipped with 1-mm pinhole collimators. 128 projections per camera, each 5 s, were acquired over 360° for each bed position with an 8 mm axial extent. Three bed positions were required to scan the neck area of the mouse. The total imaging time (micro-CT and micro-SPECT) was 38 min. Images were reconstructed using 3-dimensional ordered-subsets expectation maximization algorithm using pre-calculated system matrix into a 210 × 192 × 90 volume [20]. 20 iterations and 4 subsets were used for SPECT reconstruction. Fused reconstructed data were visualized using anatomist [21]. No attenuation and scatter corrections were performed.

2.8. Ex-vivo biodistribution studies and blood sampling

After thrombus induction (or 0.9% Nacl used as control) and radiolabeled RAM.1 injection, blood samples were obtained from tail blood sampling for blood half-life studies or were collected through left-ventricle puncture for biodistribution studies. The blood samples were weighted. Mice ($n = 5$ for each group) were sacrificed and dissected 90 min and 240 min after radiolabeled RAM.1 injection. Organs were also weighted. The radioactivity of the blood and the samples were counted on a Wallac 1470 Wizard gamma counter (Perkin Elmer, Finland). Results are represented as a percentage of injected dose per gram (%ID/g). The radioactivity of each sample was normalized to the amount of radioactivity injected and corrected from the isotope decay.

2.9. Immunofluorescence analysis of carotid thrombosis

Experiments were performed as previously published [22]. The mice ($n = 5$) were perfused with 2.5% glutaraldehyde *via* cardiac puncture in the left ventricle using a 5-ml syringe with a 25-gauge needle. An incision in the right atrium allowed to remove blood, saline, and fixative. Vessel segments were dissected and were post-fixed in 4% paraformaldehyde overnight. The carotids were washed in phosphate-buffered saline, frozen in optimal cutting temperature embedding medium, and cross-sectioned. Cryosections (8 μm) were stained for platelets using a RAM.1 antibody coupled to Alewa-488 (10 μg/ml). The samples were also stained with DAPI to detect the endothelium. A LEICA DMI 4000 B microscope (Leica Microsystem) was employed, with a Leica EL 6000 fluorescencent lamp and a 20×, 0.5 numerical aperture oil objective. Images were acquired with a Photometrics charge-coupled device (CCD) camera (CoolSNAP HQ Monochrome, Photometrics, Tucson, AZ, USA) and analyzed with ImageJ software (National Institute of Health, Bethesta, MD, USA).

2.10. Data analysis

All group of experiments were performed on 5 mice. The significance of results was assessed using an exact non-parametric Mann & Whitney test (StatXact 7.0, Cytel Inc). Non parametric statistics was used due to the small number of mice used ($p < 0.05$).

2.11. Ethicals statement

Care and use of the mice in this study follow the national guidelines approved by the ethic local committee (CREMEAS), permit No. AL/05/12/02/13.

3. Results

3.1. Binding properties of ^{99m}Tc and Hynic bound RAM.1

To ensure that coupling of Hynic and ^{99m}Tc to RAM.1 does not dramatically impair the ability of this antibody to bind to platelets, a flow cytometry approach was utilized. We observed that HYNIC-RAM.1 incubated with washed human platelets efficiently bound to platelets when compared to a control IgG (Fig. 1). Only a slight reduction in mean fluorescence intensity of HYNIC-RAM.1 was detected as compared to uncoupled control RAM.1 (Fig. 1). This indicated that coupling to Hynic and/or ^{99m}Tc does not profoundly modify the binding properties of RAM.1. After decay of Tc-99 m, [^{99g}Tc]Tc-tricine-HYNIC-labeled RAM1 was also evaluated with the same manner to check the binding capability and showed the same results as with HYNIC-RAM.1.

In vivo, the specificity of RAM.1 was tested by injection of a non-specific antibody (in our case rabbit IgG) at a high dose (50 times the amount of RAM.1 injected) right after the induction of a thrombus using $FeCl_3$. RAM.1-488 nm was injected after 30 min; we can observe that RAM.1 still labeled the thrombus (Fig. 2).

3.2. Biodistribution of [^{99m}Tc][Tc(HYNIC)-RAM.1]

Biodistribution of the radiolabeled RAM.1 was assessed 90 min and 240 min post-injection. At 90 min after injection, the highest accumulation of radioactivity, expressed as the percentage of injected dose per gram for different tissues, occurred in the spleen (95%ID/g), (Fig. 3). Significant amounts were also detected in the blood (23%ID/g), bladder

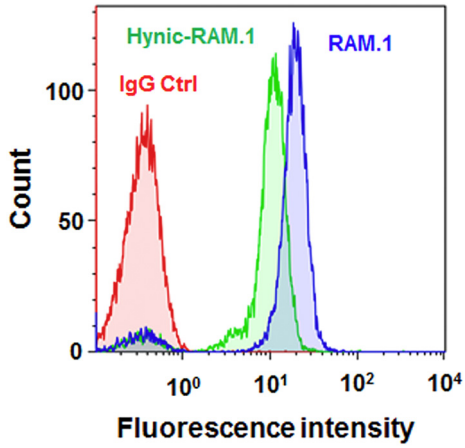

Fig. 1. Binding properties of [^{99m}Tc][Tc(HYNIC)-RAM.1]. The binding property of [^{99m}Tc][Tc(HYNIC)-RAM.1] was determined by flow cytometry using washed human platelets in comparison with unlabeled RAM.1 (10 μg/mL) and a control IgG (10 μg/mL).

(22%ID/g) and in the lung (19%ID/g). Much less radioactivity was measured in the liver (10%ID/g), heart (6%ID/g) and kidneys (4%ID/g), while only marginal amounts were detected in the skin, bones, muscles, and brain (<1%ID/g). At 240 min after injection, the spleen uptake (46%ID/g) was 50% lower than at 90 min but still much higher than the background. Besides others organs, the uptake was similar at 90 and 240 min.

3.3. In vivo detection of a forming thrombus by SPECT imaging

SPECT imaging performed around the region of $FeCl_3$-induced vessel damage was performed 90 min after *i.v.* injection of [^{99m}Tc][Tc(HYNIC)-RAM.1]. Analysis of the SPECT/CT images revealed an uptake of the radiolabeled RAM.1 at the site of injury in all injected mice ($n = 5$) (Fig. 4). This result demonstrates that [^{99m}Tc][Tc(HYNIC)-RAM.1] labeled aggregating platelets can be visualized at the site of lesion, and underscores the potential of SPECT/CT to allow detection of fresh thrombus formation in living animals. Interestingly, the uptake was concentrated at site of vessel injury and we observed only very low quantity of radioactivity in the adjacent surrounding. These results highlight the high degree of specificity of RAM.1 to detect immobilized platelets *versus* circulating platelets. To further assess the specificity of radiolabeled RAM.1, we performed a control surgical procedure by applying 0.9% NaCl to the vessel wall instead of $FeCl_3$. No thrombus was observed histologically or in SPECT-CT images (data not shown). We calculated the ratio between the radioactivity measured in the injury site (with $FeCl_3$ or 0.9% NaCl) over that in the adjacent surrounding (Fig. 5). Using $FeCl_3$, the median ratio between the thrombus and the background was 12.4 (range 9.3–42.3) as compared to 1.0 (range: 0.86–2.7) $p < 0.05$ when using 0.9% NaCl.

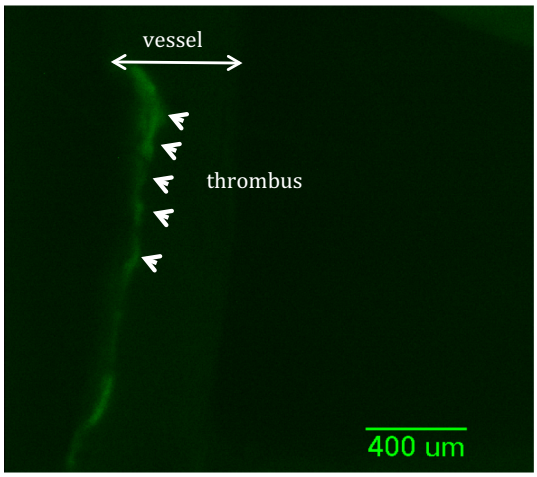

Fig. 2. RAM.1 affinity *in vivo*. Fluorescence image of RAM.1-488 nm after thrombus induction by $FeCl_3$ and injection of 500 μg of rabbit IgG (non-specific anti-body).

3.4. Histology of the thrombus

Histology and electron microscopy of FeCl3-induced injury of mouse carotid has already been described earlier [16]. Histological analysis was performed in the mice ($n = 5$) that underwent CT/SPECT imaging to show that the increase in radioactivity measured in these animals corresponded to a thrombus. Bright-field images showed that a voluminous mass was found within the lumen of mouse carotid artery (Fig. 6). Immunofluorescence staining with RAM.1 coupled to Alexa-488, confirmed that this mass was an accumulation of platelets, *i.e.* a thrombus. Staining with DAPI to identify the endothelium indicated that the formed thrombus was intraluminal.

4. Discussion

This study demonstrates a) the ability of this complex to detect a thrombus *in vivo* and b) the *in vivo* high sensitivity of the radioactive complex.

Platelets are involved in thrombus formation which can lead to life-threatening ischemic complications such as stroke and myocardial infraction. Thus, the *in vivo* follow up of platelet accumulation is of importance in order to non-invasively detect the presence of thrombi. In the present study, we developed a novel SPECT radiotracer for *in vivo* imaging. Collecting non-invasively semi-quantitative information on the expression levels of functional molecules and metabolic activities *in vivo* can be accomplished by nuclear imaging techniques such as SPECT providing a functional diagnosis with high sensitivity and good spatial resolution. We chose a nuclear imaging modality for its very high sensitivity compared to MRI or optical techniques. We used RAM.1, a monoclonal antibody which is already known to be highly specific for platelets and we coupled it to Hynic (hydrazinonicotinamide), the immunoconjugate was then radiolabeled with ^{99m}Tc. Hynic is an efficient bifunctional chelator for ^{99m}Tc used for labeling biomolecules dedicated to molecular imaging. An advantage of the HYNIC system is that it requires co-ligands to coordinate the unbound sites on the Tc, and by using various co-ligands such as tricine, ethylenediaminediacetic acid (EDDA) and glucoheptonate allowing the researcher to adjust the polarity of the molecule. It is also known that *in vitro* and *in vivo* properties of peptides and antibodies could be greatly affected by a co-ligand. The tricine formulation was already found unstable *in vitro* under diluted condition, in contrast Ono and co-workers have demonstrated that plasma proteins can stabilize Tc-99 m labeled hynic conjugated Fab fragment when tricine is used as co-ligand [23]. [^{99m}Tc][Tc(HYNIC)] radiolabeled to monoclonal antibody RAM.1 showed no decrease of immunoreactivity after radiolabeling. In addition, the targeted RAM.1 was still able to accumulate in the thrombi, generated in mouse model of acute thrombosis induced by exposure of the endothelium of the carotid artery to $FeCl_3$. The visualization of the thrombus using RAM.1 was not due to its trapping in the thrombus but to its platelet affinity. Indeed, after injection of a large amount of non-specific antibody during the thrombus formation, RAM.1 could still label the thrombus injection, 30 min after its induction. This demonstrates the very good binding affinity and retention of specificity of RAM.1. The radiolabeled RAM.1 was mainly in the spleen 90 min after injection. This result was expected since 1/3 of the platelet mass is sequestrated in this organ under normal physiological conditions.

The main factors ensuring the success of rapid imaging of thrombi relies in the ability to deliver the tracer to the thrombus with high thrombus affinity and specificity, and to select the radiotracer that can

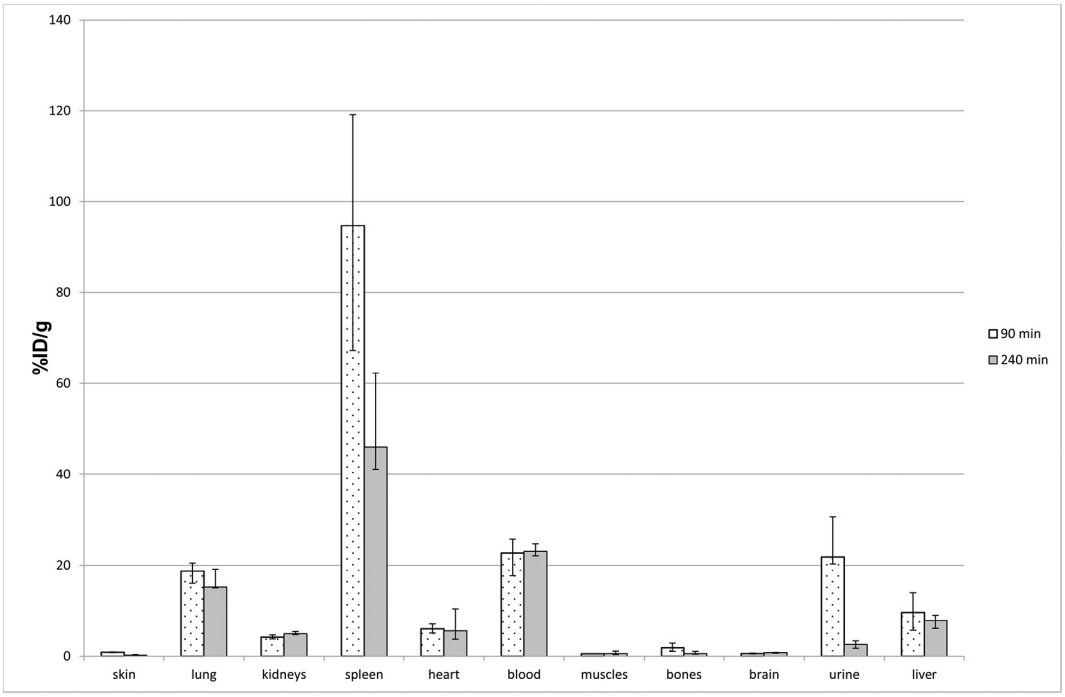

Fig. 3. Biodistribution of [^{99m}Tc][Tc(HYNIC)-RAM.1]. Radioactivity uptake in the different organs 90 min and 240 min post injection was measured using a gamma counter and expressed as percentage injected dose per gram of tissue ($n = 5$ for each group).

find the highest concentration of binding sites exposed on the thrombus with a rapid clearance of blood and muscle background. It is known that large size radiolabeled monoclonal antibodies persist in the circulation for a prolonged period of time causing a high background signal making targeted uptake difficult to distinguish. Despite relatively slow clearance from the blood, around 10 h (data not shown) which is an intrinsic problem in the use of monoclonal antibodies to develop molecular probes, [^{99m}Tc][Tc(HYNIC)-RAM.1] has a great potential as *in vivo* molecular imaging probes. Results from our studies clearly demonstrated the ability of this radioimmunoconjugate for detecting thrombi from 10 min post injection with an exceptional thrombi uptake.

Similar approaches with probes showing significant uptake in fresh thrombi without signal enhancement when used to image old thrombi have failed in the past due to the short time-window for clinical application. Main limitations of probes previously investigated in the clinic were low target-to- background ratios, slow clearance and inability to distinguish acute *versus* chronic disease [24]. For example, 99mTechnetium labeled peptide apcitide (99mTc-Acutect®), a synthetic RGD-mimicking polypeptide, which binds to glycoprotein IIb/IIIa receptors on activated platelets was approved for clinical use in 1998 for detection of acute deep vein thrombosis but was later abandoned [25].

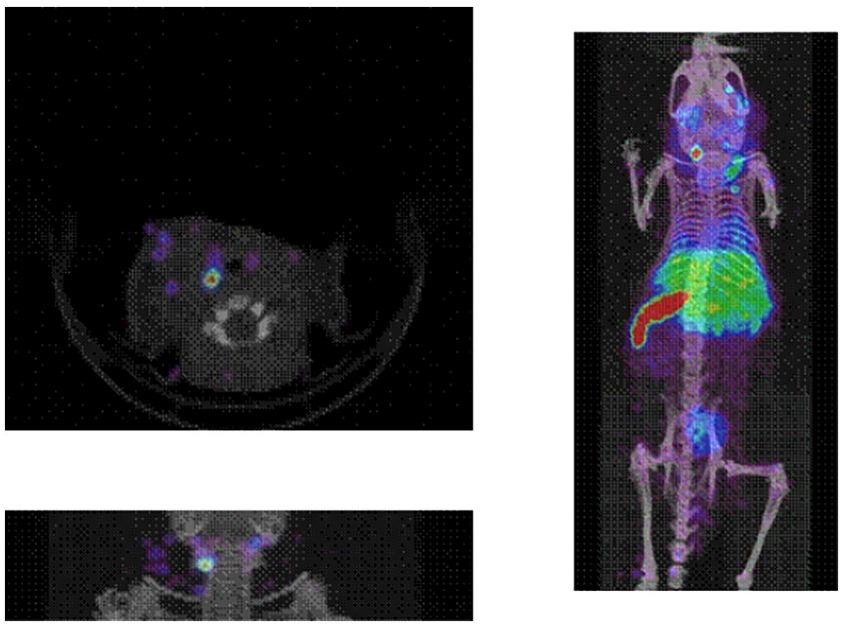

Fig. 4. Small-animal SPECT images of an *in vivo* model of mouse carotid artery thrombosis 90 min after injection of the radiotracer. Analysis of the SPECT/CT images revealed an uptake of the radiolabeled RAM.1 at the site of injury in all injected mice (n = 5).

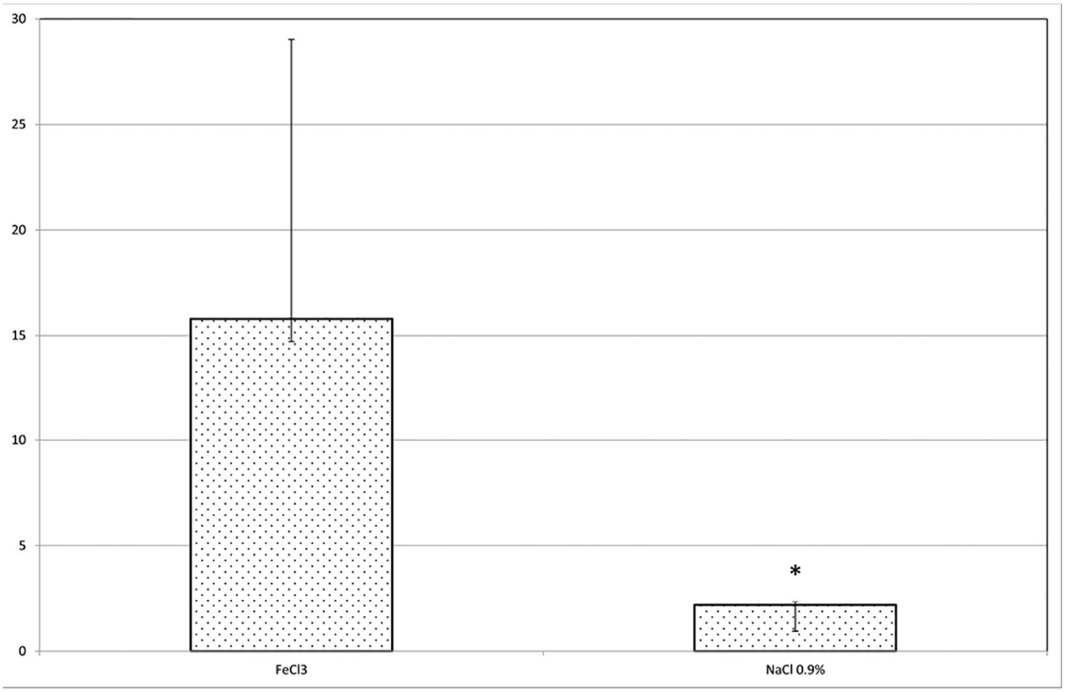

Fig. 5. Ratio between the radioactivity measured in the injury site with $FeCl_3$ or 0.9% NaCl over that in the adjacent surrounding (n = 5). Using $FeCl_3$, the median ratio between the thrombus and the background was 12.4 as compared to 1.0 when using 0.9% NaCl *Significance ($p < 0.05$).

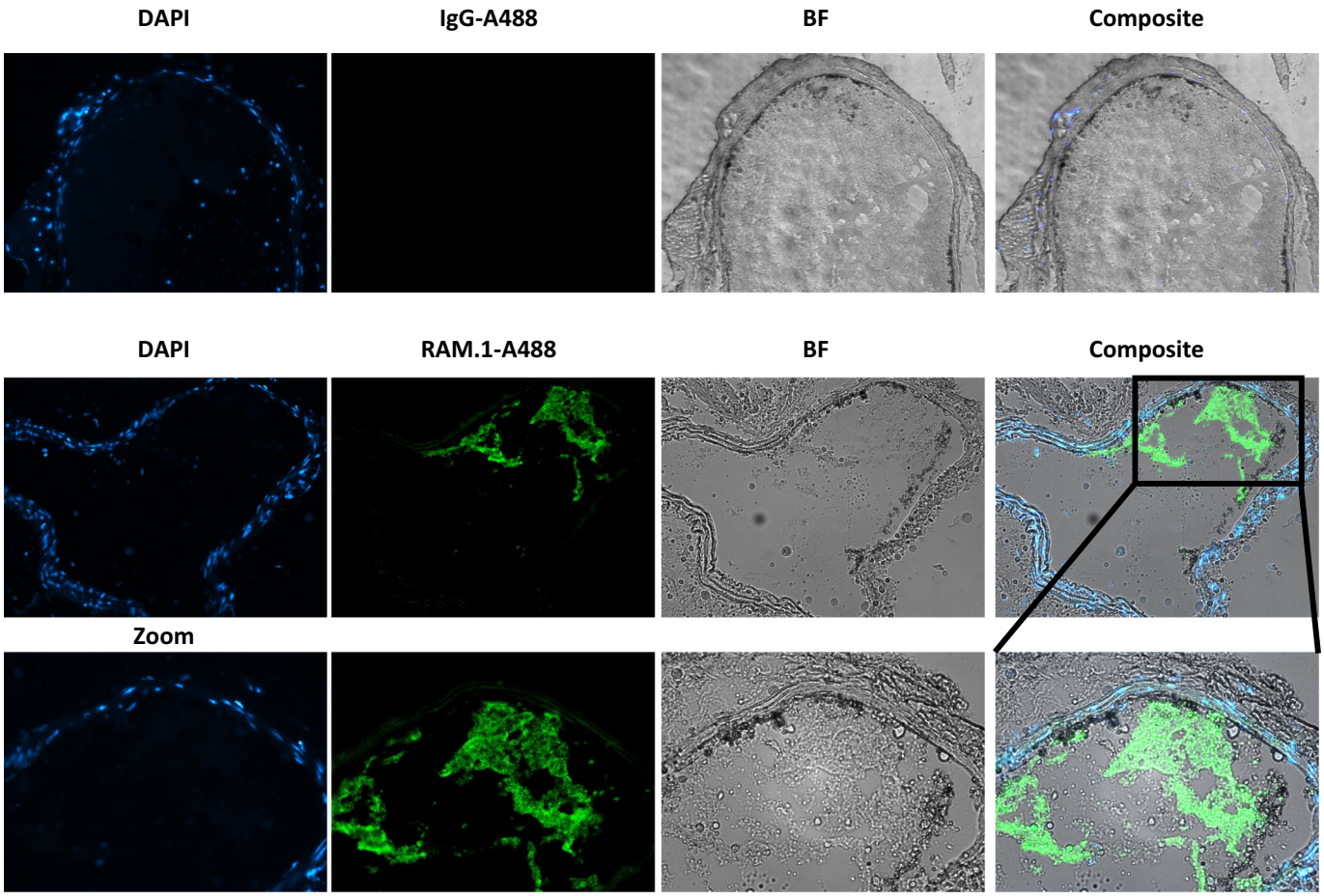

Fig. 6. Visualization of a thrombus within the carotid artery after $FeCl_3$ injury. Fluorescence (left panels) and bright field microscopic images (right panels) of the thrombus formed after $FeCl_3$-induced carotid injury in mice (n = 5) that underwent CT/SPECT imaging. Platelets forming a thrombus were detected with RAM.1 coupled to Alexa-488 and endothelial cells within the vessel wall were detected with DAPI staining. These images confirm the presence of a thrombus at a site of $FeCl_3$-injury. These images are representative of three independent experiments.

Despite a slow blood clearance and high accumulation in non-target tissues (mainly spleen, lungs, liver) radiolabeled RAM.1 represents a very useful tool to detect and image thrombus since the ratio between the signal recorded on the thrombus and the background (or contralateral signal) is important: 12.4. In other cases this ratio is between 2 and 6 [10,12,26,27]. Analysis of whole body SPECT images showed that the thrombosis area contain the highest uptake per mm^3 (even superior than the spleen).

Of note, this antibody which was developed in rats to bind mouse GPIbβ, also cross-reacts with its human counterpart, and offers the seducing opportunity to be tested in humans in future experiments.

5. Conclusion

We demonstrated that the radiolabeled RAM.1 after addition of Hynic and ^{99m}Tc was still able to recognize platelets *ex vivo*. *In vivo*, we described the high efficiency of radiolabeled RAM.1 to recognize platelet thrombi. SPECT-CT sensitivity allowed the detection and the localization of the thrombus. Because of the relative low cost and high sensitivity, these results encourage further study like the detection of non-induced thrombus and further developments toward clinical application. This is further supported by the fact that RAM.1 recognizes human platelets.

Acknowledgments

This work was supported by the Centre National de la Recherche Scientifique and the Université de Strasbourg (UMR 7178 CNRS-Université de Strasbourg). The French Institute for Research on Cancer (INCa) is gratefully acknowledged for financial support to INCa project TENPLAMET.

References

[1] Versteeg HH, Heemskerk JWM, Levi M, Reitsma PH. New Fundamentals in Hemostasis. Physiol Rev 2013;93:327–58.
[2] Jackson SP. Arterial thrombosis-insidious, unpredictable and deadly. Nat Med 2011; 17:1423–36.
[3] Michel JB, Martin-Ventura JL, Egido J. Novel aspects of the pathogenesis of aneurysms of the abdominal aorta in humans. Cardiovasc Res 2011;90:18–27.
[4] Oliveira B, Blasi F, Rietz T, Nicholas R, Caravan P. A triple-isotope SPECT/PET-CT study with two novel fibrin-specific probes for non-invasive imaging of thrombus. J Nucl Med 2015;56(Suppl. 3):465.
[5] McCarty OJT, Conley RB, Shentu WH. Molecular imaging of activated von Willebrand factor to detect high-risk atherosclerotic phenotype. JACC Cardiovasc Imaging 2010; 3:947–55.
[6] Sirol M, Aguinaldo JGS, Graham PB. Fibrin-targeted contrast agent for improvement of in vivo acute thrombus detection with magnetic resonance imaging. Atherosclerosis 2005;182:79–85.
[7] Muehlen CV, Bode C. MRI, the technology for imaging of thrombi and inflammation. Hamostaseologie 2015;35:252–62.
[8] Sampson FC, Goodacre SW, Thomas SM, van Beek EJR. The accuracy of MRI in diagnosis of suspected deep vein thrombosis: systematic review and meta-analysis. Eur Radiol 2007;17:175–81.
[9] Rouzet F, Bachelet-Violette L, Alsac JM. Radiolabeled Fucoidan as a P-selectin targeting agent for in vivo imaging of platelet-rich thrombus and endothelial activation. J Nucl Med 2011;52:1433–40.
[10] Heidt T, Deininger F, Peter K. Activated platelets in carotid artery thrombosis in mice can be selectively targeted with a radiolabeled single-chain antibody. PLoS One 2011;6:e18446.
[11] Knight LC, Romano JE. Functional expression of bitistatin, a disintegrin with potential use in molecular imaging of thromboembolic disease. Protein Expr Purif 2005; 39:307–19.
[12] Ardipradja K, Yeoh SD, Alt K. Detection of activated platelets in a mouse model of carotid artery thrombosis with F-18-labeled single-chain antibodies. Nucl Med Biol 2014;41:229–37.
[13] Perrault C, Moog S, Rubinstein E. A novel monoclonal antibody against the extracellular domain of GPIb beta modulates vWF mediated platelet adhesion. Thromb Haemost 2001;86:1238–48.
[14] Maurer E, Tang CJ, Schaff M. Targeting platelet GPIb beta reduces platelet adhesion, GPIb signaling and thrombin generation and prevents arterial thrombosis. Arterioscler Thromb Vasc Biol 2013;33:1221–9.
[15] Abrams MJ, Juweid M, Tenkate CIJ. Technetium-99m-human polyclonal igg radiolabeled via the Hydrazino nicotinamide derivative for imaging focal sites of infection in rats. J Nucl Med 1990;31:2022–8.
[16] Eckly A, Hechler B, Freund M. Mechanisms underlying FeCl3-induced arterial thrombosis. J Thromb Haemost 2011;9:779–89.
[17] Cazenave JP, Hemmendinger S, Beretz A, Sutterbay A, Launay J. Platelet-aggregation - a tool for clinical investigation and pharmacological study - methodology. Ann Biol Clin 1983;41:167–79.
[18] Koubar K, Bekaert V, Brasse D, Laquerriere P. A fast experimental beam hardening correction method for accurate bone mineral measurements in 3D CT imaging system. J Microsc 2015;258:241–52.
[19] Brasse D, Humbert B, Mathelin C, Rio MC, Guyonnet JL. Towards an inline reconstruction architecture for micro-CT systems. Phys Med Biol 2005;50:5799–811.
[20] El Bitar Z, Bekaert V, Brasse D. Acceleration of fully 3D Monte Carlo based system matrix computation for image reconstruction in small animal SPECT. IEEE Trans Nucl Sci 2011;58:121–32.
[21] Rivière D, Geffroy D, Denghien I, Souedet N, Cointepas Y. Anatomist: A python framework for interactive 3D visualization of neuroimaging data. Python in neuroscience workshop; 2011.
[22] Hechler B, Freund M, Alame G, Leguay C. The antithrombotic activity of EP224283, a Neutralizable dual factor Xa inhibitor/glycoprotein IIbIIIa antagonist, exceeds that of the Coadministered parent compounds. J Pharmacol Exp Ther 2011;338:412–20.
[23] Ono M, Arano Y, Mukai T, Fujioka Y, Ogawa K, Uehara T, et al. (^{99}m)Tc-HYNIC-derivatized ternary ligand complexes for (^{99}m)Tc-labeled polypeptides with low in vivo protein binding. Nucl Med Biol 2001;28:215–24.
[24] Houshmand S, Salavati A, Hess S, Ravina M, Alavi A. The role of molecular imaging in diagnosis of deep vein thrombosis. Am J Nucl Med Mol Imaging 2014:406–25.
[25] Lister-James J, Knight LC, Maurer AH, Bush LR, Moyer BR, Dean RT. Thrombus imaging with a technetium-^{99}m-labeled activated platelet receptor-binding peptide. J Nucl Med 1996;37:775–81.
[26] Boros E, Rybak-Akimova E, Holland JP. Pycup-a bifunctional, cage-like ligand for Cu-64 radiolabeling. Mol Pharm 2014;11:617–29.
[27] Ay I, Blasi F, Rietz TA, Rotile NJ. In vivo molecular imaging of thrombosis and thrombolysis using a fibrin-binding positron emission tomographic probe. Circ Cardiovasc Imaging 2014;7:697–705.